

Filamentous Crystal Growth In Organic Liquids And Selection Of Crystal Morphology

Takumi Yashima

Tokyo Metropolitan University

Marie Tani

Tokyo Metropolitan University

Rei Kurita (✉ kurita@tmu.ac.jp)

Tokyo Metropolitan University

Article

Keywords:

Posted Date: March 18th, 2022

DOI: <https://doi.org/10.21203/rs.3.rs-1456190/v1>

License: © ⓘ This work is licensed under a Creative Commons Attribution 4.0 International License.

[Read Full License](#)

Filamentous crystal growth in organic liquids and selection of crystal morphology

Takumi Yashima, Marie Tani and Rei Kurita*¹

¹*Department of Physics, Tokyo Metropolitan University,
1-1 Minamioosawa, Hachioji-shi, Tokyo 192-0397, Japan*

(Dated: March 16, 2022)

Filamentous crystals such as whisker crystals are often seen not only in metallic liquids, but also in organic liquids and solutions. They are interested as reinforce materials. However, it remains challenging to induce filamentous crystals due to an incomplete understanding of the mechanisms behind their formation. In this paper, we investigate filamentous crystal growth in viscous organic liquids. It is found that filamentous crystals grow via an extraordinary dynamical path, where the molecules locally evaporate to bubbles and then redeposit to the tip of growing crystalline filaments. We also succeeded in controlling whether filamentous or faceted crystal growth is selected by inducing or suppressing the bubbles.

Crystalline materials form the base of most of the functional electronics, making the development of new crystals a focal point for research over the years [1–4]. The electronic states and physical characteristics of crystals are not only determined by microscopic crystal structure, but also by macroscopic morphology, as seen in topological effects [3], the alignment of carbon nanotubes [5], and polymer crystals [4, 6]. An example of this is the monocrystalline whisker: whiskers are single, defect-free filaments of materials [7–9]. Whisker crystals can be ubiquitously seen in many materials, for example, in metallic liquids such as zinc and tin [7], in fullerenes [8], and even in organic viscous liquids [9]. It is known that whiskers have their high tensile strength and that whisker of the fullerenes is stable to the electron beam irradiation [8]. Though whiskers are potentially useful, the growth of whiskers may also induce failure in the insulation of electronic equipment. In order to gain control over crystal morphology, it is necessary to understand the mechanism by which they form.

It seems that mechanism of filamentous crystal growth depends on the systems. In metallic system, filamentous crystal usually grows from the crystal base and it induces by mechanical stress [7]. Meanwhile, the filamentous crystal growth of salts with impurities or with gypsum occurs by anisotropic concentration effect [10, 11]. Interestingly, the whisker of the fullerene is induced at a liquid-liquid interface between two solvents [8]. In addition, the filamentous crystal growth has been observed instead of faceted crystal growth in supercooled viscous liquids such as *o*-terphenyl (OTP) and indomethacin in certain temperature ranges [9]. Although whisker crystals are by no means rare, the mechanism behind filamentous crystal growth is not yet fully understood.

Here, we investigate the mechanism behind filamentous crystal growth in organic liquids, OTP and salol, and propose a new way to control crystal morphology. It is found that filaments grow via an extraordinary dynamical pathway i.e. through the formation of bubbles. Furthermore, we report success in artificially controlling the morphology, switching from filaments to faceted crys-

tals, by suppressing the bubbles.

RESULTS

Filamentous crystal growth in OTP

We start with microscopy observation of filamentous crystal growth in OTP. Figures 1(a)-(d) show the crystal growth of OTP at 283 K. While the crystal front grows, it is often the case that there is a bubble located between the liquid and the crystal i.e. the black droplet seen in Fig. 1(a). A filamentous crystal goes on to form which follows the bubble's movement [Fig. 1(b)-(d)]. It is worth noting that the filamentous crystal growth is faster than the bulk crystal growth. Figure 1(e) shows the temperature dependence of the growth rate of OTP V . The red filled circles show the growth rate in the bulk region (without bubbles), while the squares show the growth rate of the filamentous crystal (with bubbles). The growth rate is obtained by averaging over 5 different points, either on the tip of different filaments or on a growth front. The temperature dependence of the growth rate in bulk is bell-shaped and seems to be consistent with classical theory [1, 2]. Meanwhile, it is remarkable that the growth rate V of the filaments remains almost constant between 283 K and 298 K. This suggests that the growth of filaments with bubbles only weakly depends on the viscosity. We note that these bubbles are stable at the tip of the crystal over the range 283 K \sim 298 K. Above 298 K, bubbles appear at grain boundaries in the interior of the crystals and are trapped inside. On the other hand, below 283 K, the number of bubbles decreases significantly and disappear in a few seconds even if they appear (the filled squares).

Here, it should be clarified whether the filamentous crystal grows and causes the bubble to appear, or vice versa. Bubbles emerge during crystallization and often remain in the liquid phase after the crystal is melted above the melting point. When this is quenched again to the crystallization temperature and pre-existing faceted

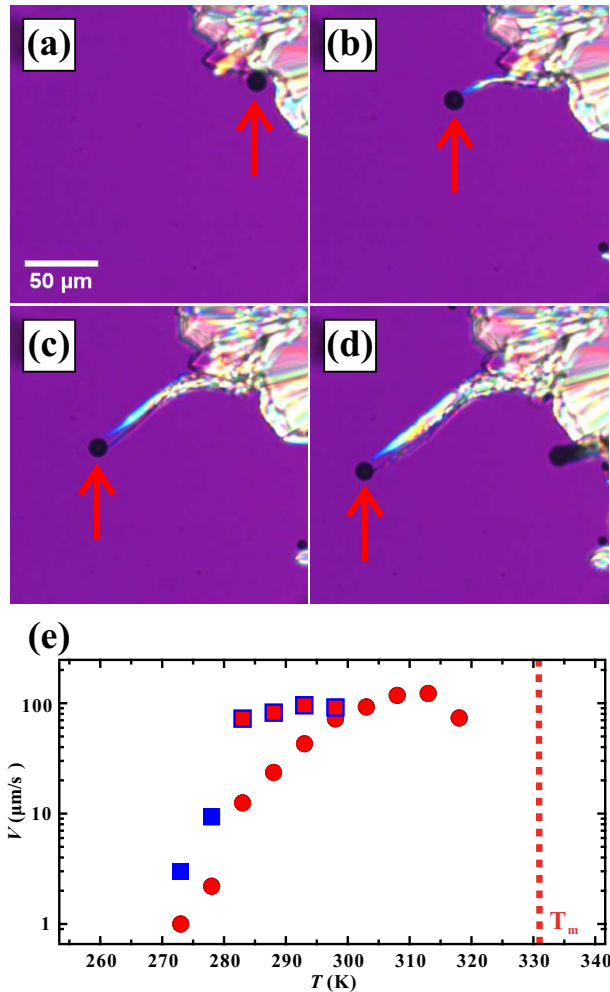


FIG. 1. Microscopy observation of filamentous crystal growth in OTP at 283 K. (a) $t = 27.0$ s, (b) 28.0 s, (c) 29.0 s, and (d) 30.0 s. The arrow indicates the bubble which induces filamentous crystal growth. (e) The growth rate of the OTP crystal as a function of temperature. Filled circles correspond to crystal growth in bulk. Open squares correspond to filamentous growth with the stable bubble, while filled squares correspond to filamentous growth with the unstable bubble. V is obtained by averaging over 5 points; the errors in V are smaller than the symbol size. The growth rate of the filamentous crystal with the bubble (open squares) remains almost constant between 283 K and 303 K, although V in the bulk (filled circles) decreases due to the viscosity. It is found that the filamentous crystal growth rate suddenly decreases when the bubbles are unstable.

crystals start growing in bulk, the growth front makes contact with these bubbles, initiating filamentous crystal growth (Movie S1). We note that the bubble also starts moving just after contact with the growing crystal interface. In observations of such situations, we can confirm the crystal growth rate is similar to the rate of filament growth when bubbles were found already at crystal interfaces, like for the velocities denoted by the open squares

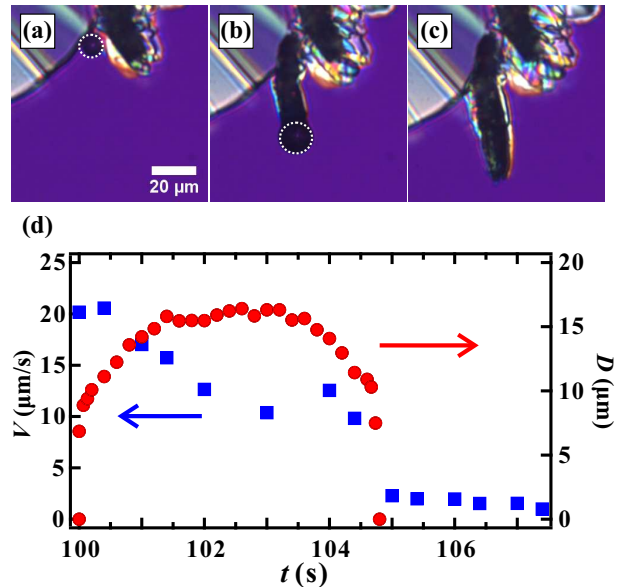


FIG. 2. Microscopy observation of filamentous crystal growth in OTP at 278 K. (a) $t = 100.0$ s, (b) 103.0 s, and (c) 105.5 s. The dotted line indicates the bubble, which induces filamentous crystal growth. (d) The time evolution of the growth rate of the filamentous crystal (squares) and the diameter of the bubble (circles). The bubble disappears at $t = 105.5$ s; the growth rate also suddenly decays toward the bulk growth rate.

in Fig. 1(e). Thus, it seems that the remaining bubbles are the same bubbles which spontaneously appear during the initial crystal growth. In addition, it is found that the bubbles are not stable at 278 K. Figures 2(a)-(c) show the microscopy images at 278 K. A small bubble appears with some radius at $t = 100.0$ s. This size is maintained for several seconds before the bubble disappears [Fig. 2(c)]. Figure 2(d) shows the time evolution of the bubble radius and crystal growth rate. The crystal growth rate is faster than that in bulk, but it suddenly decreases after the bubble disappears. These results suggest that it is in fact the bubble that is inducing filamentous crystal growth.

We go on to investigate the origin of the bubbles. The possibility of air dissolved in the liquid is considered first. We mixed air bubbles into the sample beforehand and observed the crystal growth after a faceted crystal interface makes contact with an air bubble (Movie S2). The size of the air bubble is similar to that of the bubble shown in Fig. 1. In the case of the air bubble, the faceted crystal growth simply continues, with no filaments seen. This means that the bubbles which emerged during crystal growth are not composed of air.

Another possibility is a bubble of gas phase OTP. The bubbles appear at grain boundaries in the interior of the crystal. Since OTP has a large density difference be-

tween liquid and crystal [12], the density of the liquid at the interface decreases, especially at the grain boundary. Thus, cavitation can occur due to the negative pressure [13, 14]. This scenario is consistent with the fact that most bubbles disappear when the crystal melts. It is also consistent with the disappearance of bubbles at lower temperature (Fig. 2). If the bubble is gas phase OTP, it is natural to think that OTP molecules are deposited onto the crystal surface from the bubble, while molecules are simultaneously transferred from the liquid to the bubble via evaporation. In this case, the position of the bubble center changes due to deposition and evaporation. This position change would be induced in an Ising-like manner rather than a diffusive manner; this is consistent with the fact that the velocity of the bubble, which is equal to the growth rate of the filamentous crystal growth, is less dependent on the viscosity.

Filamentous crystal growth in the capillary tube

If this is correct, it should be possible for filamentous crystals to grow even if the liquid and the crystal are not in contact with each other. Figure 3 shows the time evolution of the crystal growth when OTP was placed in a capillary tube with inner diameter 0.13 mm at $T_x = 283$ K. The bubble fills the diameter of the capillary tube and hinders contact between the liquid and the crystal. Although the crystal is not in contact with the liquid, it was observed that the crystal keeps growing. Remarkably, the growth rate is $100.6 \mu\text{m/s}$, which is close to the filamentous crystal growth rate [Fig. 1(e)]. Here, we cannot rule out the possibility that the liquid and the crystal are in slight contact. However, the area of contact between the crystal and the liquid is clearly smaller than that in the experiment using a sample confined by flat cover glasses. Since the crystallization rate is unchanged even in the capillary tube, we conclude that the molecules are supplied to the crystal interface through a bubble or layer of gas phase OTP.

Suppression of filamentous crystal growth by impurity

In the course of the investigation, we also considered the suppressing of the bubble formation by adding a small amount of impurities. We mixed a small amount of organic solvent (toluene or acetone) with OTP as an impurity. Since the OTP crystal cannot include the solvent, the impurity is ejected to the outer liquid phase. Figure 4 shows the crystal growth at 293 K in (a) pure OTP, (b) OTP with 1.0 wt% toluene, and (c) OTP with 1.0 wt% acetone. We note that the melting temperature and the glass transition temperature are unchanged when such small amounts of impurities are mixed with OTP. Thus,

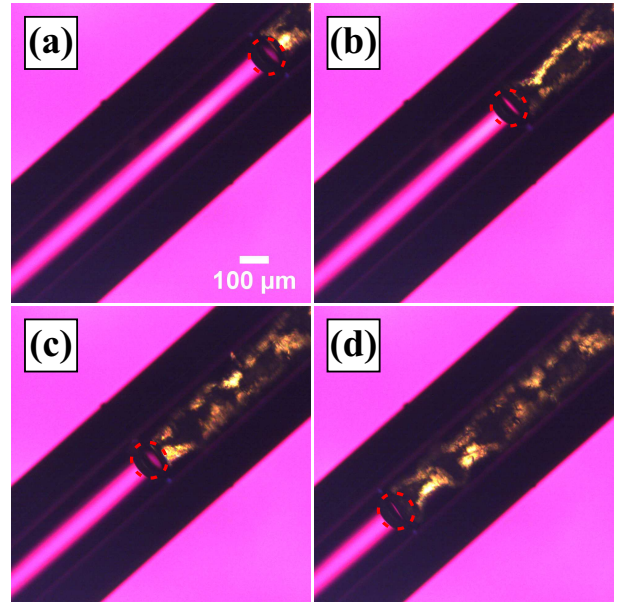


FIG. 3. Crystal growth for OTP in a capillary tube with inner diameter 0.13 mm at $T_x = 283$ K. (a) $t = 95.7$ s, (b) 98.7 s, (c) 101.7 s, and (d) 104.7 s. The dotted lines show the positions of the bubble. Although the crystal is not in contact with the liquid, it was observed that the crystal keeps growing. It is also remarkable that the growth rate is $100.6 \mu\text{m/s}$, which is close to the filamentous crystal growth rate [see also Fig. 1(e)].

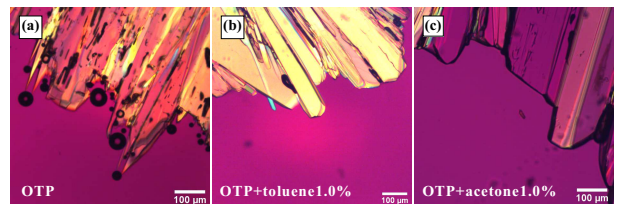


FIG. 4. Crystal morphologies in (a) pure OTP, (b) OTP with 1 wt% toluene, and (c) OTP with 1 wt% acetone at 283 K. Filamentous crystal growth with bubbles is observed in pure OTP; when a small amount of toluene or acetone is mixed in, there are no bubbles and only faceted crystal growth is observed.

it is expected that the viscosity is also unchanged. Compared with observations in pure OTP, the number of the bubbles is significantly reduced. It is expected that the density change becomes smaller at the grain boundary since solvent molecules are accumulated near the crystal growth front, suppressing cavitation. Then, faceted crystal growth is only observed when OTP is mixed with impurities.

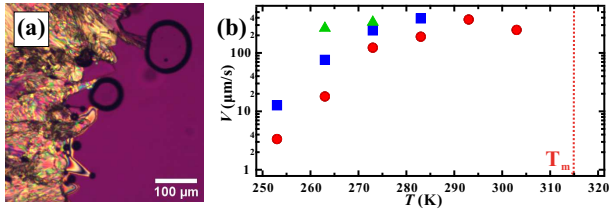


FIG. 5. (a) An image of the filamentous crystal growth in salol at 273 K. (b) The growth rate of the salol crystal. Circles, triangles, and squares correspond to the crystal growth in bulk, with the large bubble ($> 100 \mu\text{m}$), and with the small bubble ($\sim 40 \mu\text{m}$), respectively. V of the filamentous crystal growth with the bubble is much larger than that in bulk.

Filamentous crystal growth in salol

Note that the mechanisms proposed above may be ubiquitous at least in organic liquids. Thus, to see whether this phenomenon is ubiquitous in organic liquids, we also investigated crystal growth in salol, finding again that filamentous crystal growth occurs through bubbles shown as in Fig. 5. Figure 5(a) shows a snapshot during the filamentous crystal growth at 273 K and it is found that the filamentous crystal is growing followed by the bubble movement similar to the crystal growth in OTP system. Furthermore, it is found that the growth is faster when the bubble size is larger. Here we note that both OTP and salol have large density difference between liquid and crystal [12]. Thus this filamentous crystal growth might be occurred ubiquitously when the density difference between liquid and crystal is large.

DISCUSSION

Here, we discuss physical factors for the filamentous crystal growth rate. The growth rate of the filamentous growth may be determined both by the deposition rate onto the crystal surface from the bubble and the evaporation rate from the liquid to the bubble. In this dynamical path, the diffusion in liquid can be ignored and it is consistent that the filamentous crystal growth rate is independent with the viscosity. The bubbles are stable when the deposition rate is balanced to the evaporation rate, while they are unstable if the deposition rate is larger than the evaporation rate [15]. Figure 1 shows that the filamentous crystal growth rate suddenly decreases when the bubbles are unstable. This reason has been unclear yet, thus it is an important future work.

To confirm the stability of the bubbles in bulk, we checked for filamentous crystal growth in an open system where the OTP liquid is dropped on a cooled substrate. Bubbles are also generated in the open system, with filamentous crystal growth following bubble movement (see

Movie S3). Here we note that a bubble can be stable in a liquid even though a size of the bubble is nanoscale although mechanism of the stability of the nano bubbles in the liquid has been unclear yet [15–18]. Consequently, when a gas bubble is designedly injected into a super-cooled liquid, the bubble remains for a long time and it may induce the filamentous crystal growth. In addition, the bubble becomes more stable near a thermodynamical triple point. It is expected that the filamentous crystal growth frequently occurs.

Finally, we also observed that the bubble motion is not straight but often curved. The filamentous crystal growth follows the bubble, making bent filaments. Here we discuss the possible reasons as to why bubble motion is often curved during the crystal growth. As the OTP molecules are evaporated from the liquid and deposited on the crystal on the other side of the bubble, a large temperature gradient is generated inside the bubble due to latent heat [19, 20]. Any inhomogeneities in the temperature profile would misalign the gradient from the growth direction of the filament, causing the bubble to veer off in a different direction (see Movie S4). In addition, when a bubble is in contact with two filaments, we observe that it moves in a straight, stable path. When one of the two filaments separates from the bubble, the straight motion becomes unstable, and the trajectory starts to curve. All of these bubble dynamics can be explained through an evaporation/deposition mechanism for crystal growth.

CONCLUSION

To summarize this study, we investigated the mechanism behind filamentous crystal growth in OTP and salol. It was found that bubbles of OTP gas induce filamentous growth. The dynamical pathway is highly out of the ordinary, consisting of evaporation from the liquid to the bubble and subsequent deposition from the bubble to the crystal interface. The mechanism is directly demonstrated in a capillary tube. In addition, by mixing a small amount of an organic solvent such as toluene or acetone, the generation of bubbles is suppressed and filament growth is prevented: this shows that crystal morphology can be selected by mixing (removing) an organic solvent. These results provide new insights into the science of crystal growth. Since a bubble can be generally stable in a liquid, it is expected that the filamentous growth can be ubiquitously induced by injecting the gas bubble designedly. In addition, the findings will progress understanding the crystal growth near a thermodynamical triple point. Furthermore, the results in this paper will greatly contribute to engineering applications such as improving the stability of insulation material, forming crystalline nanowires, and accelerating crystal growth.

MATERIALS AND METHODS

We used o-terphenyl (OTP) with a purity of 99 % purchased from Sigma-Aldrich and phenyl salicylate (salol) with a purity of 98.0 % purchased from Wako Pure Chem. Ind. The melting temperatures T_m of OTP and salol are 331.0 K and 315.0 K, respectively. An OTP or salol sample was sandwiched between two cover glasses; the sample thickness was set to 25 μm using spacers. The sample was sealed with UV curable glue to prevent air influx and evaporation. The temperature of the sample was controlled using a temperature controller (LINKAM, 10002L). Samples of OTP were quenched to 293 K at 20 K/min, allowing it to completely crystallize. These were heated to T_m , where the crystal slowly melted. With a part of the crystal still undissolved, the sample was quenched to a crystallization temperature T_x at 20 K/min. Observation of the samples was initiated at a time $t = 0$, when the temperature reached T_x . Note that the undissolved crystalline portions acted as nuclei for growth. The process was observed using a polarizing microscope (Nikon ECLIPSE LV100ND) with a retardation plate; note that the images captured are purple when the sample does not show birefringence. For additional impurities, toluene with a purity of 99.0 % purchased from Wako Pure Chem. Ind. and acetone with a purity of 99.0 % purchased from Wako Pure Chem. Ind. were mixed with OTP and stirred well.

ACKNOWLEDGMENTS

M. T. was supported by JSPS KAKENHI (20K14431) and R. K. was supported by JSPS KAKENHI (20H01874).

AUTHORS CONTRIBUTIONS

R. K. conceived the project and T. Y. performed the experiment. T. Y., M. T. and R. K. conceived the crystal growth mechanism. T. Y. and R. K. wrote the manuscript.

COMPETING INTERESTS

The authors declare that they have no competing financial interests.

CORRESPONDENCE

Correspondence and requests for materials should be addressed to R.K. (kurita@tmu.ac.jp).

All data generated or analysed during this study are included in this published article and its supplementary information files.

-
- [1] A. Pimpinelli and J. Villain, *Physics of Crystal Growth* (Cambridge University Press, Cambridge, UK, 1999).
 - [2] P. G. Debenedetti, *Metastable Liquids* (Princeton Univ. Press, Princeton, 1997).
 - [3] N. Nagaosa and Y. Tokura, *Nat. Nanotechnol.* **8**, 899 (2013).
 - [4] D. Bi, C. Yi, J. Luo, J.-D. Décoppet, F. Zhang, S. M. Zakeeruddin, X. Li, A. Hagfeldt, and M. Grätzel, *Nat. Energy* **1**, 1 (2016).
 - [5] C. Bower, W. Zhu, S. Jin, and O. Zhou, *Appl. Phys. Lett.* **77**, 830 (2000).
 - [6] S. Kimata, T. Sakurai, Y. Nozue, T. Kasahara, N. Yamaguchi, T. Karino, M. Shibayama, and J. A. Kornfield, *Science* **316**, 1014 (2007).
 - [7] J. J. Petrovic, J. V. Milewski, D. L. Rohr, and F. D. Gac, *J. Mater. Sci.* **20**, 1167 (1985).
 - [8] K. Miyazawa, Y. Kuwasaki, A. Obayashi, and M. Kuwabara, *J. Mater. Res.* **17**, 83 (2002).
 - [9] Y. Sun, L. Zhu, K. L. Kearns, M. D. Ediger, and L. Yu, *Proc. Natl. Acad. Sci. USA* **108**, 5990 (2011).
 - [10] Q. Guan, W. Sun, Y. Hu, Z. Yin, and C. Guan, *Scientific Reports* **7**, 7085 (2017).
 - [11] H. Fu, J. Huang, L. Shen, Y. Li, L. Xu, F. Wei, J. Li, and G. Jiang, *Crystal Growth & Design* **18**, 6694 (2018).
 - [12] T. Konishi and H. Tanaka, *Phys. Rev. B* **76**, 220201(R) (2007).
 - [13] K. Morinaga, N. Oikawa, and R. Kurita, *Sci. Rep.* **8**, 12503 (2018).
 - [14] K. Morinaga, M. Tani, and R. Kurita, *Phys. Rev. Research* **2**, 013098 (2020).
 - [15] K. Yasui, T. Tuziuti, W. Kanematsu, and K. Kato, *Langmuir* **32**, 11101 (2016).
 - [16] F. R. Young, *Cavitation* (Imperial College Press, London, 1999).
 - [17] R. Okamoto and A. Onuki, *Eur. Phys. J. E* **38**, 72 (2015).
 - [18] R. Okamoto and A. Onuki, *J. Phys.:Condens. Matter* **28**, 244012 (2016).
 - [19] A. Onuki, *Phase Transition Dynamics* (Cambridge Univ. Press, Cambridge, 2002).
 - [20] A. Onuki and K. Kanatani, *Phys. Rev. E* **72**, 066304 (2005).

Supplementary Files

This is a list of supplementary files associated with this preprint. Click to download.

- [MovieS1.mov](#)
- [MovieS2.mov](#)
- [MovieS3.mov](#)
- [MovieS4.mov](#)